Lifetime measurement in neutron-rich A~100 nuclei

Ansari, S.; Régis, J.-M.; Jolie, J.; Saed-Samii, N.; Warr, N.; Korten, W.; Zieliska, M.; Salsac, M.-D.; Blanc, A.; Jentschel, M.; Köster, U.; Mutti, P.; Soldner, T.; Simpson, G.S.; Drouet, F.; Vancraeyenest, A.; de France, G.; Clément, E.; Stezowski, O.; Ur, C.A.; Urban, W.; Regan, P.H.; Podolyák, Zs.; Larijani, C.; Townsley, C.; Carroll, R.; Wilson, E.; Mach, H.; Fraile, L.M.; Paziy, V.; Olaizola, B.; Vedia, V.; Bruce, A.M.; Roberts, O.J.; Smith, J.F.; Scheck, M.; Kröll, T.; Hartig, A.-L.; Ignatov, A.; Ilieva, S.; Lalkovski, S.; Mrginean, N.; Otsuka, T.; Shimizu, N.; Togashi, T.; Tsunoda, Y.

Published in:
EPJ Web of Conferences

DOI:
10.1051/epjconf/201819305003

Published: 14/11/2018

Document Version
Publisher's PDF, also known as Version of record

Lifetime measurement in neutron-rich A∼100 nuclei

S. Ansari[1,2⋆], J-M. R*é*gis[2], J. Jolie[2], N. Saed-Samii[2], N. Warr[2], W. Korten[1], M. Zielińska[1], M.-D. Salsac[1], A. Blanc[3], M. Jentschel[3], U. Köster[3], P. Mutti[3], T. Soldner[3], G.S. Simpson[4], F. Drouet[4], A. Vancraeyenest[4], G. de France[5], E. Clément[5], O. Stezowski[6], C.A. Ur[7], W. Urban[8], P.H. Regan[9,10], Zs. Podolyák[9], C. Larijani[9,10], C. Townsley[9], R. Carroll[9], E. Wilson[9], H. Mach[11⋆⋆], L.M. Fraile[12], V. Paziy[12], B. Olaizola[12,13], V. Vedia[12], A.M. Bruce[14], O.J. Roberts[14], J.F. Smith[15], M. Scheck[15], T. Kröll[16], A.-L. Hartig[16], A. Ignatov[16], S. Ilieva[16], S. Lalkovski[17], N. Mărginean[18], T. Otsuka[19,20,21,22], N. Shimizu[19], T. Togashi[19], Y. Tsunoda[19]

[1] *CEA, Université Paris-Saclay, IRFU, 91191 Gif-sur-Yvette, France*
[2] *Institute für Kernphysik der Universitat zu Koeln, Zuelpicher Str. 50937 Koeln, Germany*
[3] *Institut Laue-Langevin, 71 avenue des Martyrs, 38042 Grenoble Cedex, France,*
[4] *LPSC, 53 avenue des Martyrs, 38026 Grenoble Cedex, France,*
[5] *Grand Accélérateur National d'Ions Lourds (GANIL), CEA/CRF-CNRS/IN2P3, 14076 Caen Cedex 05, France,*
[6] *IPN de Lyon, 4, Rue Enrico Fermi, 69622 Villeurbanne Cedex, France,*
[7] *INFN, via Marzolo 8, 35131 Padova, Italy,*
[8] *Faculty of Physics, University of Warsaw, ul. Pasteura 5, 02-093, Warsaw, Poland,*
[9] *Department of Physics, University of Surrey, Guildford GU2 7XH, United Kingdom,*
[10] *National Physical Laboratory, Teddington, Middlesex, TW11 0LW, United Kingdom,*
[11] *National Centre for Nuclear Research, Andrzeja Sołtana 7, 05-400 Otwock-Świerk, Poland,*
[12] *Grupo de Fisica Nuclear, FAMN, Universidad Complutense, 28040 Madrid, Spain,*
[13] *TRIUMF, 4004 Wesbrook Mall, Vancouver, BC, V6T 2A3, Canada.*
[14] *School of Computing, Engineering and Mathematics, University of Brighton, Brighton, BN2 4GJ, United Kingdom,*
[15] *School of Engineering and Computing, University of the West of Scotland, High Street, Paisley, PA1 2BE, United Kingdom,*
[16] *Institut für Kernphysik, TU Darmstadt, Schlossgartenstr. 7, 64289 Darmstadt, Germany,*
[17] *Faculty of Physics, University of Sofia, 1164 Sofia, Bulgaria,*
[18] *Horia Hulubei NIPNE, 77125 Bucharest, Romania,*
[19] *Center for Nuclear Study, University of Tokyo, Hongo, Bunkyo-ku Tokyo 113-0033, Japan,*
[20] *Department of Physics, University of Tokyo, Hongo, Bunkyo-ku Tokyo 113-0033, Japan,*
[21] *NSCL, Michigan State University, East Lansing, Michigan 48824, USA,*
[22] *Instituut voor Kern- en Stralingsfysica, KU Leuven, B-3001 Leuven, Belgium.*

Abstract. Lifetimes of excited states of the ^{98,100,102}Zr nuclei were measured by using the Generalized Centroid Difference Method. The nuclei of interest were populated via neutron-induced fission of ^{241}Pu and ^{235}U during the EXILL-FATIMA campaign. The obtained lifetimes were used to calculate the B(E2) transition strengths and β deformation

⋆ *Present address:* saba.ansari@cea.fr
⋆⋆ Deceased

parameters which were then compared with the recent theoretical predictions obtained with Monte Carlo Shell Model.

1 Introduction

Nuclei in the phase transition region at A∼100 have been a topic of research in nuclear structure physics for many years. Neutron rich nuclei in this mass region show a large, stable deformation and exhibit many interesting structural phenomena. The island of quadrupole deformation appearing beyond N=60 in the A∼100 mass region has first been observed in the 1960s by S.A.E. Johansson [1] in a study of γ rays emitted by fission fragments. Shortly after, Cheifetz et al [2] identified excited states and measured lifetimes in A∼100 nuclei using spontaneous fission of ^{252}Cf, reporting a rotational-like behavior of neutron-rich even-even Zr, Mo, Ru and Pd isotopes, consistent with theoretical predictions of Refs [3, 4].

In Zr isotopes the energy of the 2_1^+ state decreases dramatically at the transition point N=60. Experimental studies also show that for N $\geq$ 60, the E(4^+)/E(2^+) ratio is larger than 3, which is characteristic of a well deformed rotor [5–8]. These studies give a direct indication towards the much speculated sudden increase in absolute transition strength from ^{98}Zr to ^{100}Zr, but due to the lack of information on the low-lying states of ^{98}Zr, this has not yet been fully established.

The shape change phenomenon may be explained by the strong p-n interaction between proton $\pi 1g_{9/2}$ and neutron $\nu 1g_{7/2}$ subshells. The protons are excited from the predominantly filled $\pi p_{1/2}$ shell to the predominantly empty $\pi g_{9/2}$ shell [9] which leads to the decrease in the spin-orbit coupling in the neutron sector and reduces the shell gap between $\nu g_{7/2}$ and $\nu d_{5/2}$. As the occupation of the $\nu g_{7/2}$ neutron orbital increases, the spin-orbit splitting increases in the proton sector, reducing the energy gap between $\pi p_{1/2}$ and $\pi g_{9/2}$. This self-stabilizing process is responsible for the appearance of the deformation in Zr isotopes.

The monopole part of the p-n interaction causes the dramatic lowering of the 0_2^+ state (from 1.58 MeV to 0.85 MeV) as soon as two neutrons are added to the $\nu 2d_{5/2}$ orbital i.e., as we go from ^{96}Zr (empty $\nu 2d_{5/2}$) to ^{98}Zr [10]. The lowering of this configuration continues in ^{100}Zr where it becomes the 0_1^+ state of ^{100}Zr, while the spherical ground state of ^{98}Zr becomes the non-yrast 0_2^+ state (0.331 MeV) lying right above the 2_1^+ state of ^{100}Zr (0.212 MeV). This makes ^{100}Zr a perfect shape transitional point as beyond N≥60, the energy of the 0_2^+ state increases significantly and only one regular rotational band is observed for ^{102}Zr at low excitation energy.

A similar behavior is observed in the Sr isotopic chain where the reduced transition strengths measured in both Coulomb excitation [11] and lifetime studies [13] suggest a quantum phase transition at N=58 and shape coexistence between highly-deformed prolate and spherical structures in ^{98}Sr. Additionally, a low mixing between the coexisting structures in ^{98}Sr was determined [11, 12]. In order to understand how the shape transition proceeds in the Zr isotopes, we have performed a new lifetime measurement. Such measurements are crucial to determine transition strengths which gives the systematic information on nuclear deformation and collectivity.

2 Lifetime measurement

The experimental set up at the Institut Laue-Langevin (ILL) Grenoble, France consisted of 8 EX-OGAM Clovers and 16 cerium doped $LaBr_3$ detectors arranged in a compact configuration around the ^{241}Pu and ^{235}U targets to perform γ-ray spectroscopy following neutron-induced fission. Lifetimes of the low-lying excited states of ^{98,100,102}Zr were obtained using the Generalized Centroid Difference

Method (GCDM) [14] for the sub-nanosecond region and the slope method for the long-lived ones (≥1 ns), independently for each target. In this work we will discuss the lifetime measurement of the 2_1^+ states of ^{98,100,102}Zr using the 2_1^+ lifetime in ^{100}Zr extracted from data obtained with the ^{241}Pu target, as an example.

The lifetime of the 2_1^+ state of ^{100}Zr was measured using the GCDM which is given as [13]:

$$\triangle C_{FEP} = \triangle C_{exp} + \frac{1}{2}\Big[\frac{(\triangle C_{exp} - \triangle C_{BG})}{p/b}\Big]_{\text{feeder}} + \frac{1}{2}\Big[\frac{(\triangle C_{exp} - \triangle C_{BG})}{p/b}\Big]_{\text{decay}}, \quad (1)$$

and

$$\tau = \frac{1}{2}(\triangle C_{FEP} - PRD) \quad (2)$$

where $\triangle C_{FEP}$ is the centroid difference between the delayed and anti-delayed time distributions related only to the Full Energy Peaks events, $\triangle C_{exp}$ is the measured centroid difference, which also includes the contribution from the background events (as shown in Fig. 1), $\triangle C_{BG}$ is the centroid difference related only to the background, p/b is the peak-to-background ratio and PRD is the Prompt Response Difference, which describes the complete time-walk of the set-up. The first (second) background correction term of Eq. 1 is related to the feeding (decay) transition in a spectrum gated on the decay (feeding) transition, and hence at the reference energy (E_{ref}). Determination of the PRD curve is necessary to correct the obtained lifetime from the time-walk effect as well as to minimize the systematic errors. The complete description of the procedure to obtain the PRD curve can be found in Ref. [15].

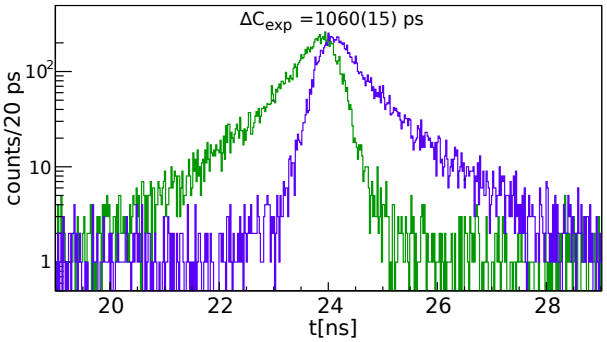

Figure 1: Delayed and anti-delayed time distributions for the lifetime measurement of the 2_1^+ state of ^{100}Zr.

The lifetime analysis for the 2_1^+ level of ^{100}Zr is described in Figs. 2 and 3. Fig. 2a shows that in a fission experiment the γ-ray spectrum includes numerous γ-ray transitions from various fission fragments as well as Compton background. Having the FATIMA array combined with EXOGAM Ge detector array provides the additional advantage of using a Ge gate to select the nucleus of interest. This further improves the p/b ratio, especially in case of a complex γ-ray spectrum where the $LaBr_3$ energy resolution is not sufficient to separate the transitions. The decay energy (497 keV) of the $6_1^+ \rightarrow 4_1^+$ transition of ^{100}Zr was used as a Ge gate to select the nucleus of interest and in accordance with Eq. 1, the reference energy gate was applied separately to the energies of the decay ($2^+ \rightarrow 0^+$,

212 keV) and feeding ($4^+ \rightarrow 2^+$, 352keV) transitions. The double-gated Ge and $LaBr_3$ spectra can be seen in Fig. 2a for the reference energy at 212 keV ($2_1^+ \rightarrow 0_1^+$) and in Fig. 3a for the reference energy at 352 keV ($4_1^+ \rightarrow 2_1^+$). The reliability of GCDM procedure is related to its mirror symmetric character and the fact that both the feeding and decay transitions are used to evaluate the lifetime. Since the background makes a non-negligible contribution to the measured centroid centroid (Fig. 1), it is necessary to do background correction. Figs. 2b and 3b shows the background correction procedure. This is performed by:

1. calculating the centroid difference between the delayed and the anti-delayed time distribution ($\triangle C_{BG}$) at few background positions (shown by dashed lines in Fig 2b) in the vicinity of the FEP,

2. fitting these $\triangle C_{BG}$ points using a polynomial function (green curve in Fig. 2b) and reading the background correction value ($\triangle C_{BG}$) at the FEP position to correct for the lifetime as per Eq. 1.

3. determining the p/b ratio from the doubly-gated $LaBr_3$ spectrum (Figs. 2a and 3a).

The same procedure is applied when the reference energy gate is at the feeding transition and the decay transition is the FEP as shown in Fig. 3. Since the reference energy is then at the feeder of the state, the background region is different and so are the background gates. It must be noted that as the reference energy is flipped from decay to feeder, both the background curve and the PRD curve are inverted in Fig. 2b as compared to Fig. 3b. The time-walk correction is directly read from the PRD curve where, $PRD_{E_{decay}}(E_{feeder})$ is same as -$PRD_{E_{feeder}}(E_{decay})$. The Eqs. 1 and 2 were applied to the values listed in Fig. 2b and 3b, yielding a lifetime of 830(30) ps. The same procedure was applied for ^{235}U target yielding a lifetime of 850(20) ps. Finally, an average of the lifetimes obtained from both data sets has been adopted for the 2_1^+ level of ^{100}Zr and is given as 840(18) ps. The lifetime measurement of the short-lived 2_1^+ state of ^{98}Zr was also attempted using GCDM, however due to uncertainties in the PRD and Compton-background correction only an upper limit of 6 ps was obtained. The long lifetime of the 2_1^+ state of ^{102}Zr was measured using the slope method and a result of 2.91(8) ns was obtained.

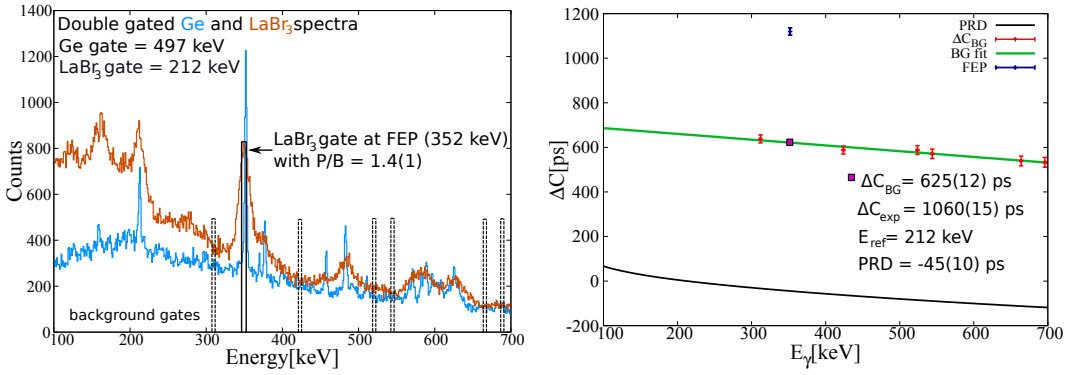

(a) (b)

Figure 2: Lifetime measurement using the GCDM for the 2_1^+ state of ^{100}Zr, E_{ref} set at decay transition ($2_1^+ \rightarrow 0_1^+$, 212 keV). The centroid difference between the delayed and anti-delayed is measured at the background points (dashed lines in (a)) which is then plotted (red points) in (b). The PRD curve (solid black curve in (b)) is shifted vertically such that the PRD at E_{ref} is 0 ps.

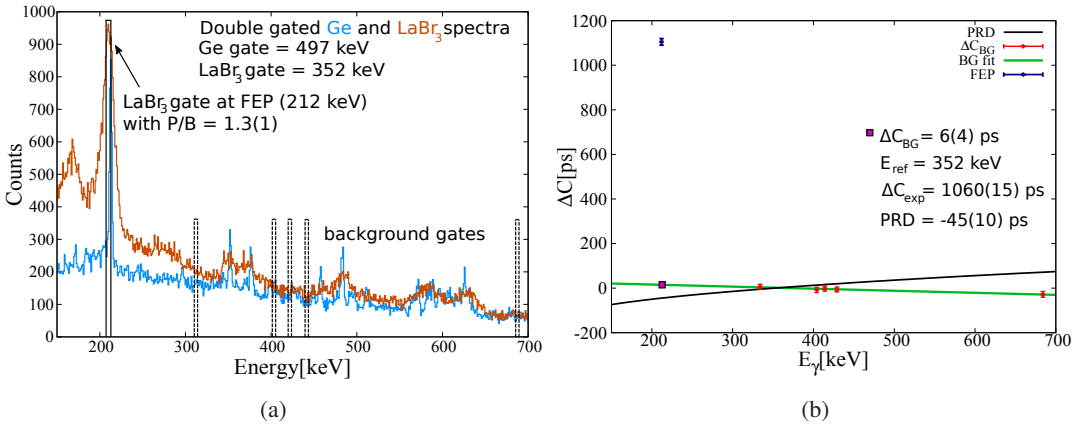

(a) (b)

Figure 3: Lifetime measurement using the GCDM for the 2_1^+ state of ^{100}Zr, E_{ref} set at the feeding transition ($4_1^+ \rightarrow 2_1^+$, 352keV).

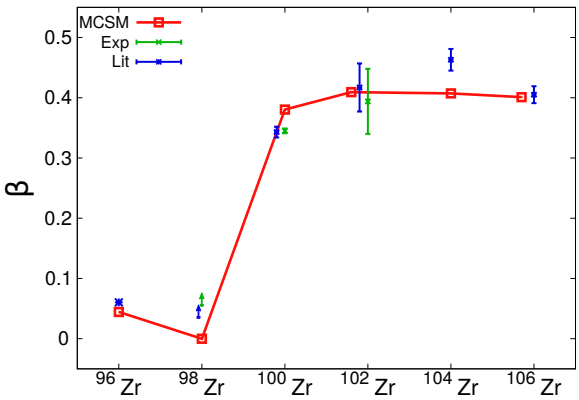

Figure 4: Evolution of the β deformation parameter (from Table. 1) of the 2_1^+ level in the Zr isotopic chain. The present experimental results (shown in green) are compared with the literature values [5, 6, 17–24] as well as the theoretical MCSM calculations [16].

3 Results and Discussion

The lifetimes can be used to evaluate the B(E2, ↑) transition strengths and the β deformation parameters using the following equations [17]:

$$\tau = 40.81 \times 10^{13} E^{-5} [B(E2) \uparrow / e^2 b^2]^{-1} (1 + \alpha)^{-1}, \tag{3}$$

and

$$\begin{aligned} \beta =& (4\pi/3ZR_0^2)[B(E2) \uparrow / e^2]^{1/2}, \\ R_0^2 =& 0.0144A^{2/3} \end{aligned} \tag{4}$$

where α is the total internal coefficient, τ is the lifetime in ps and E is the transition energy in keV. The results are presented in Table 1. The comparison of thus determined experimental deformation parameter (β) with those resulting from state-of-the art Monte Carlo Shell Model calculations [16] is shown in Fig. 4. The MCSM foresees a dramatic change in the deformation parameter at ^{98}Zr with a large deformation beyond N = 60. Also, the sudden decrease in the energy of the 2_1^+ level and the transition strength from ^{98}Zr to ^{100}Zr is well reproduced by the MCSM calculations. The lower limit on the deformation parameter at ^{98}Zr does not allow a meaningful comparison between the experimental results and the theory. Therefore further study of the lifetimes in ^{98}Zr is essential to establish a possible phase shape transition at N=60 in the Zr chain.

Table 1: Transition strength and deformation parameters for the 2_1^+ levels in the Zr chain. "Exp" denotes to the values obtained using the lifetime measured in the present work, while "Lit" refers to earlier measurements [5, 6, 17–24]. B(E2) values are expressed in e^2b^2.

Nuclei	B(E2)↑(Exp.)	β(Exp.)	B(E2)↑(Lit.)	β(Lit.)
^{96}Zr	-	-	0.0303(36)	0.0604(11)
^{98}Zr	≥0.0245	≥0.0535	≥0.0095	≥0.0333
^{100}Zr	1.045(22)	0.345(4)	1.031(52)	0.343(9)
^{102}Zr	1.402(385)	0.394(54)	1.57(30)	0.417(40)
^{104}Zr	-	-	1.978(155)	0.463(18)
^{104}Zr	-	-	1.554(105)	0.405(14)

Acknowledgement

The EXILL&FATIMA campaign would not have been possible without the support of several services at the ILL and the LPSC. We are grateful to the EXOGAM collaboration for the loan of the detectors, to GANIL for assistance during installation and dismantling, and to the FATIMA collaboration for the provision of $LaBr_3$ (Ce) detectors and analogue electronics. This work was supported by German BMBF under grant 05P15PKFNA and 05P12PKNUF and by the UK Science and Technology facilities council and the UK National Measurement Office. Theoretical studies including the MCSM calculations were supported in part by JSPS Grants-in-Aid for Scientific Research (23244049), in part by HPCI Strategic Program (hp150224), in part by MEXT and JICFuS and Priority Issue on Post-K computer (Elucidation of the fundamental laws and evolution of the universe) (hp160211), and by the CNS-RIKEN joint project for large-scale nuclear structure calculations.

References

[1] S.A.E. Johansson, Nuclear Physics, **64**, (1965) 147.
[2] E. Cheifetz, R. C. Jared, S. G. Thompson and J. B. Wilhelmy, Phys. Rev. Lett., **25**, (1970) 38.
[3] D.A. Arseniev, A. Sobiczewski and V.G. Soloviev, Nuclear Physics A, **139**, (1969) 269.
[4] R.K. Sheline, I. Ragnarsson and S.G. Nilsson, Physics Letters B, **41**, (1972) 115.
[5] A. G. Smith, R. M. Wall, D. Patel, G. S. Simpson, D. M. Cullen, J. L. Durell, S. J. Freeman et al., Journal of Physics G: Nuclear and Particle Physics **28**, (2002) 2307.
[6] L. Bettermann, J.-M. Régis, T. Materna, J. Jolie, U. Köster, K. Moschner *et al.,* Phys. Rev. C. **82**, (2010) 044310.
[7] A.G. Smith, D. Patel, G.S. Simpson, R.M. Wall, J.F. Smith, O.J. Onakanmi, I. Ahmad and J.P. Greene *et al.,* Physics Letters B, **591**, (2004) 55.
[8] K. Heyde and J. L. Wood, Reviews of Modern Physics **83**, (2011) 1467.
[9] P. Federman, S. Pittel and A. Etchegoyen, Physics Letters B, **140**, (1984) 269.
[10] T. Otsuka and Y. Tsunoda, Journal of Physics G: Nuclear and Particle Physics **43**, (2016) 024009.
[11] E. Clément, M. Zielińska, S. Péru, H. Goutte, S. Hilaire, A. Görgen, W. Korten *et al.,* Phys. Rev. C **94**, (2016) 054326.
[12] E. Clément, M. Zielińska, A. Görgen, W. Korten, S. Péru *et al.,* Phys. Rev. Lett. **116**, (2016) 022701.
[13] J.-M. Régis, J. Jolie, N. Saed-Samii, N. Warr *et al.,* Phys. Rev. C. **95**, (2017) 054319, Erratum: **95**, 069902.
[14] J.-M. Régis, G. Pascovici, J. Jolie and M. Rudigier, Nuclear Instruments and Methods in Physics Research Section A **622**, (2010) 83.
[15] J.-M. Régis, G.S. Simpson, A. Blanc, G. de France, M. Jentschel, U. Köster, P. Mutti *et al.,* Nuclear Instruments and Methods in Physics Research Section A **763**, (2014) 210.
[16] T. Togashi, Y. Tsunoda, T. Otsuka and N. Shimizu, Phys. Rev. Lett. **117**, (2016) 172502.
[17] S. Raman, C.W. Nestor and P. Tikkanen, Atomic Data and Nuclear Data Tables **78**, (2001) 1.
[18] H. Mach, M. Moszyǹski, R.L. Gill, F.K. Wohn, J.A. Winger, J. C. Hill, G. Molnár and K. Sistemich, Physics Letters B. **230**, (1989) 21.
[19] H. Ohm, M. Liang, G. Molnar, K. Sistemich, Z.Phys. **A334**, (1989) 519.
[20] G. Lhersonneau, H. Gabelmann, N. Kaffrell, K. -L. Kratz, B. Pfeiffer and the ISOLDE Collaboration, Z.Phys. **A332**, (1989) 243.
[21] F. Browne, A.M. Bruce, T. Sumikama, I. Nishizuka, S. Nishimura, P. Doornenbal et al., Physics Letters B **750**, (2015) 448.

[22] G. Kumbartzki, N. Benczer-Koller, J. Holden, G. Jakob, T.J. Mertzimekis, M.J. Taylor, K.-H. Speidel, R. Ernst, A.E. Stuchbery, C.W. Beausang and R. Krücken, Physics Letters B. **562**, (2003) 193.

[23] E. Cheifetz, H. A. Selic, A. Wolf, R. Chechik and J. B. Wilhelmy, *Proc., Conf. on Nuclear Spectroscopy of fission Products, Grenoble, France, 1979*, (1980) 193.

[24] R. C. Jared, H. Nifenecker and S. G. Thompson, *Physics and Chemistry of Fission 1973*, (1974) 211.